



## Three-dimensional metallic photonic crystals fabricated by soft lithography for midinfrared applications

Jae-Hwang Lee,<sup>a)</sup> Chang-Hwan Kim, Yong-Sung Kim, and Kai-Ming Ho  
Ames Laboratory, Department of Physics and Astronomy, Iowa State University, Ames, Iowa 50011

Kristen Constant  
Ames Laboratory; and Department of Materials Science and Engineering, Iowa State University, Ames, Iowa 50011

Cha Hwan Oh  
Department of Physics, Hanyang University, Seoul 133-791, South Korea

(Received 11 October 2005; accepted 23 March 2006; published online 3 May 2006)

We present an efficient method of fabricating freestanding three-dimensional metallic photonic crystals using soft lithography. Low cost and ease of fabrication are achieved through gold sputter deposition on a freestanding woodpile polymer template. We compare experimental results to theoretical calculations for tetragonal and face-centered-tetragonal structures as a function of the number of layers. The photonic crystals behave like full metallic structures with a photonic band edge at a wavelength of  $3.5 \mu\text{m}$ . The rejection rates of the structures are about 10 dB/layer. © 2006 American Institute of Physics. [DOI: 10.1063/1.2201621]

Since the proof<sup>1</sup> of the existence of photonic crystals, which can prohibit the propagation of light in all directions at a certain range of frequencies<sup>2,3</sup> called a photonic band gap (PBG), researchers have intensively investigated easier fabrication methods. As PBGs approach the optical range, semiconductor processing has emerged as a reliable means of achieving large-area structures with superior fidelity and intentional defects.<sup>4,5</sup> However, achieving PBG effects requires that the thickness be increased significantly, which is both costly and tedious using semiconductor processing techniques. On the other hand, one interesting alternative, direct laser writing using two-photon polymerization, seems to have the capability of fabricating highly layered structure even with nonperiodic functional defects.<sup>6,7</sup> However, the lateral area of available photonic crystals (PhCs) is practically limited to an order of  $10^{-2} \text{ mm}^2$  because registration of structures usually relies on high-resolution piezoelectric actuators. Meanwhile, attempts to use metals in place of dielectric materials have continued and have shown some interesting properties, for example, high quality factors for cavities,<sup>8</sup> robust photonic band gaps,<sup>9</sup> extrinsically tailored absorption,<sup>10</sup> selectively enhanced thermal radiation,<sup>11</sup> and recently, negative refraction.<sup>12</sup> Metallic photonic crystals (MPCs), however, have not been intensively explored for optical applications compared to planar metallic structures such as frequency selective surfaces,<sup>13–15</sup> because of the difficulties and high cost of three-dimensional (3D) microfabrication. In applications, the midinfrared (mid-IR) range is a significantly important spectral window in material identification, thermal imaging, and gas analysis in commercial, observational astronomy and defense.<sup>16</sup> More specifically, recent analytic chemistry and biochemistry may require optical elements compatible with microfluidic systems, often fabricated by soft lithographic techniques,<sup>17</sup> for lab-on-a-chip applications. As new demands have emerged in mid-IR applications, MPCs have received growing attention, and alternative fabrication methods for MPCs are required.

In this letter we report an efficient method employing soft lithography to fabricate freestanding 3D MPCs for midinfrared ranges without undesirable optical effects resulting from a substrate such as reflection and absorption. Since our approach is nonoptical replica molding, in principle, the structural resolution can follow the highest resolution of the two-dimensional (2D) lithography used in the master pattern fabrication, while 3D photolithographic techniques such as direct laser writing and holographic lithography have an optical limit in spatial resolution especially vertically.<sup>18</sup> Because metallic PhCs can demonstrate functionality with fewer layers than dielectric PhCs,<sup>10</sup> wider structures are preferred over taller structures. We achieved  $\text{mm}^2$ -wide four-layer MPCs with a metallic photonic band edge. Figure 1 shows the schematic procedure for fabrication of the MPCs. First, we spin coat at 4000 rpm a water-soluble polymer on a glass substrate to form a sacrificial layer. Commercially available glue (O'Glue,<sup>®</sup> Itoya) was used for the water-soluble polymer with mixing ratio of water to glue of 2:1 by weight. We used a soft lithographic technique, called two-polymer microtransfer molding<sup>19</sup> to fabricate a polymer structure layer by layer. In the technique, a photocurable prepolymer (J-91, Summers Optical) is filled in the microchan-

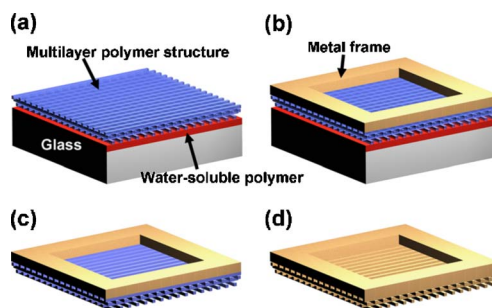


FIG. 1. (Color online) A schematic procedure for fabrication of a four-layer freestanding metallic photonic crystals. (a) A polymer structure on a substrate coated with a water-soluble layer. (b) A rigid metal frame is attached around the polymer structure. (c) The polymer structure is separated from the substrate by dissolving the water-soluble layer. (d) The freestanding polymer structure is converted to a metallic structure by the sputter coating of gold.

<sup>a)</sup>Electronic mail: leejh@iastate.edu

nels of an elastomeric mold, and solidified. A second photocurable prepolymer (SK-9, Summers Optical) is selectively coated on the filled polymer as a bonding material. The adhesive prepolymer is cured after making contact with the substrate. The filled polymer structure is left on the substrate by peeling off the elastomeric mold. A multilayer structure is fabricated by repeating the same processes, as shown in Fig. 1(a). In our experiments, the polymer structure consists of layers of equally spaced polymer rods,  $1.2\ \mu\text{m}$  wide and  $1.1\ \mu\text{m}$  high, with a periodicity of  $2.5\ \mu\text{m}$ . The orientation of each layer is perpendicular to the layer below. For the perpendicular alignment of the first and the second layers, alignment marks were used. A diffracted moiré fringe based alignment technique, in which the fringes are monitored at the angle of the first-order diffraction corresponding to the periodicity of polymer rods, was used to align the third and fourth layers parallel to the first and second layer, respectively.<sup>20</sup> As shown in Fig. 1(b), a 0.2 mm thick brass frame was attached on the multilayer polymer structure with the photocurable prepolymer (J-91, Summers Optical). This frame improves the rigidity of the structure after separation from the substrate. The framed structure was submerged in distilled water for 1 h to dissolve the water-soluble layer. When removing the separated structure from water, the plane of the structure was perpendicular to the water-air interface to minimize damage due to the surface tension of water. The freestanding structure was dried in an oven at  $60\ ^\circ\text{C}$  for 24 h. After drying, the freestanding polymer structure was fairly flat although the suspended area is quite large ( $3.5 \times 3.5\ \text{mm}^2$ ). Gold was used as coating material since it has excellent optical properties for IR applications<sup>21</sup> and is chemically inert. In Fig. 1(d), gold was deposited by sputter coating with a tilted rotation to reduce inhomogeneity.

Since sputter deposition is not conformal for 3D microstructures, we qualitatively characterized the deposition of gold optically as increasing thickness of gold. To make a gradient in the thickness, half of a four-layer freestanding polymer template was covered by an aluminum mask apart from the surface of the template about 0.5 mm. The deposition thickness was 150 nm, which is overabundant for an even surface since the skin depth  $d$  of gold is below 15 nm for mid-IR from 2 to  $10\ \mu\text{m}$ , obtained from the equation,  $d = \lambda_0 / (4\pi\kappa n)$ ,<sup>22</sup> where  $n$  and  $\kappa$  are the refractive index and extinction coefficient of gold, respectively, and  $\lambda_0$  is the wavelength of light in vacuum. Sputter deposition was performed on both sides of the template under a pressure of 80 mtorr of argon. We measured normal transmittance and reflectance of several areas along the direction from a covered area to a fully exposed area using a Fourier transform infrared (FTIR) microscope (Hyperion 1000, Bruker) with a sampling area of  $90 \times 90\ \mu\text{m}^2$ . Figures 2(a) and 2(b) show reflectance and transmittance spectra of the selected areas having different gold deposition thicknesses. As the deposition thickness of gold increases, reflectance approaches unity at the wavelengths longer than a photonic band edge of  $3.5\ \mu\text{m}$ . The corresponding transmittance spectra drop down to the measurement limit of the spectrometer in the band gap. The band gap effects appear first at longer wavelengths due to smaller skin depths for longer wavelengths. For partially coated areas, intrinsic absorption peaks from the polymer structure still appear, which are identifiable by the absorption spectrum of the structural polymer J-91, measured by a FTIR spectrometer (Magna 760, Nicolet), in Fig. 2(c). Even

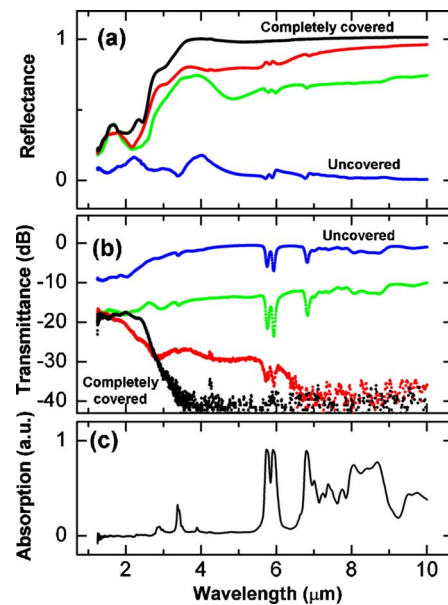


FIG. 2. (Color online) (a) Reflectance and (b) transmittance spectra of a four-layer freestanding structure are characterized with increasing thickness of gold. (c) Absorption spectrum of a homogeneous thin film of the structural polymer J-91 is presented.

though local structures of each measured site are not identical, this gives qualitative information to determine the deposition thickness. These measurements show that 150 nm is enough to convert a polymer structure to a metallic structure.

We fabricated gold-coated two-, three-, and four-layer freestanding structures. In Figs. 3(a) and 3(b), scanning electron microscopy (SEM) micrographs of a fabricated four-layer structure show two coexisting crystal structures in a single sample, tetragonal and face centered tetragonal (FCT), respectively. The visible transmission image in Fig. 3(c) shows domains because the intensity of transmitted visible light is mostly proportional to the openings in local structures. The brightest and darkest areas represent tetragonal and FCT structures. Although the deformation due to the flexibility of the elastomeric mold in fabrication would limit the size of a single domain in a multilayered structure, the

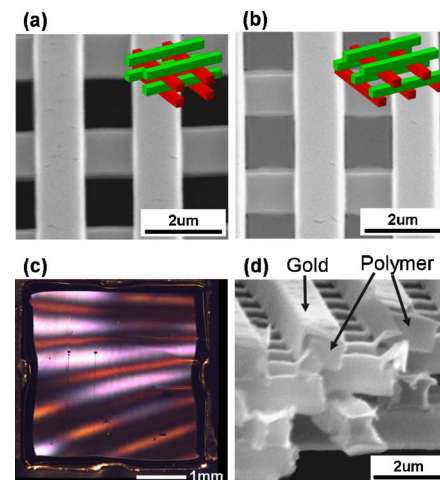


FIG. 3. (Color online) Top-view SEM micrographs of (a) tetragonal and (b) face-centered-tetragonal domains in a freestanding gold-coated four-layer structure are shown with corresponding schematics. Moiré fringes in (c) a transmission optical image show the domains of the four-layer structure. (d) Well-covered gold layers are shown in the cross section of a four-layer structure.



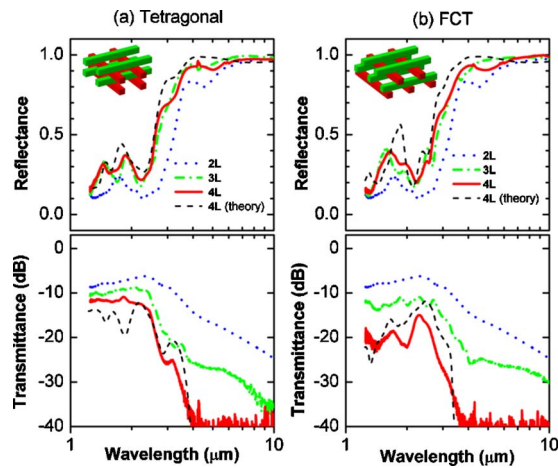


FIG. 4. (Color online) Reflectance and transmittance spectra of tetragonal and FCT structures as increasing the number of layers are shown with results of numerical calculations for four-layer metallic structures.

observed moiré fringes indicate that the size is large enough for optical applications (on the order of  $\text{mm}^2$ ). Figure 3(d) is the cross section of a four-layer structure to evaluate the results of the gold deposition for a complex geometry in parallel with the optical means shown in Fig. 2. Since we deposited no additional gold after cutting the structure, the exposed polymer structure can be differentiated from the gold layer in brightness and its different deformation behavior at the breaking point. From the cross section, we can infer that the polymer structures were covered completely with gold by the sputter coating.

We measured reflectance and transmittance of two different structures, tetragonal and FCT, as a function of the number of layers. Figure 4 shows the results with those of numerical calculations. In the calculations, the analytic modal expansion method combined with a transfer-matrix technique<sup>23</sup> was used to simulate solid gold structures. Reflectance spectra for both tetragonal and FCT structures show similar characteristics except in the shorter wavelength region below  $2.5 \mu\text{m}$ . In transmission, a typical metallic band gap is observed for wavelengths longer than  $3.5 \mu\text{m}$ . The rejection factors within the gap is around 10 dB/layer for both structures; however, the transmission window of the tetragonal structure is more clearly defined due to higher flat transmittance than that of the FCT structure below  $2.5 \mu\text{m}$ . The transmission contrasts (defined as transmittance out of gap divided by transmittance in gap) for four-layer tetragonal and FCT are approximately 30 and 20 dB. The experimental results show good agreement with the numerical calculations, in which solid gold structure are assumed, and this means that the thickness of the gold-coated structure is sufficiently bigger than the skin depth for the system to behave as a solid gold structure. We also observed that high order diffractions exist when wavelengths are shorter than  $3 \mu\text{m}$  with an angle-resolved FTIR spectroscopy. Since an objective mirror of the FTIR microscope has a finite acceptance angle of  $30^\circ$ , the light emerging over the angle is not counted as signals. Therefore the actual reflectance and transmittance at wavelengths shorter than  $3 \mu\text{m}$  are higher than the measured values in Fig. 4. To simulate the actual measurements, we assumed that a focused beam of the FTIR microscope has multiple wave vectors satisfying the condition,  $\sin \theta \geq \sqrt{k_x^2 + k_y^2} / |\mathbf{k}|$ , where  $k_x$ ,  $k_y$  and  $\theta$  are the two orthogonal wave vector components parallel to a surface of a photonic

crystal and the acceptance angle, respectively. Transmission and reflection contributions for higher order diffracted beam are included in our calculations only when the diffracted beam falls within the acceptance angle.

In summary, we developed an efficient method for free-standing 3D MPCs using soft lithography. The nonoptical nature of the method yields excellent 3D definition in fabrication of templates. By a simple deposition process, the polymer templates are converted to MPCs exhibiting fully metallic features with a high rejection factor and high transmission contrast in spite of their complex geometry. With a high degree of control over the structure of MPCs, this fabrication method will allow us to implant defect structures to tailor optical functionalities without modification of the fabrication method. The structural flexibility of the MPCs will allow applications requiring curved geometries. Moreover, the distinct freestanding feature, if fluid permeable, would be useful for combining photonics and microfluidics in biological and chemical engineering.

This work is supported by the Director for Energy Research, Office of Basic Energy Sciences. The Ames Laboratory is operated for the U.S. Department of Energy by Iowa State University under Contract No. W-7405-Eng-82. One of the authors (C.H.O.) acknowledges the Korea Science and Engineering Foundation through the quantum photonic Science Research Center for financial support.

- <sup>1</sup>K. M. Ho, C. T. Chan, and C. M. Soukoulis, *Phys. Rev. Lett.* **65**, 3152 (1990).
- <sup>2</sup>E. Yablonovitch, *Phys. Rev. Lett.* **58**, 2059 (1987).
- <sup>3</sup>S. John, *Phys. Rev. Lett.* **58**, 2486 (1987).
- <sup>4</sup>S. Y. Lin, J. G. Fleming, D. L. Hetherington, B. K. Smith, R. Biswas, K. M. Ho, M. M. Sigalas, W. Zubrzycki, S. R. Kurtz, and J. Bur, *Nature (London)* **394**, 251 (1998).
- <sup>5</sup>S. Noda, K. Tomoda, N. Yamamoto, and A. Chutinan, *Science* **289**, 604 (2000).
- <sup>6</sup>H.-B. Sun, S. Matsuo, and H. Misawa, *Appl. Phys. Lett.* **74**, 786 (1999).
- <sup>7</sup>V. Mizeikis, K. K. Seet, S. Juodkazis, and H. Misawa, *Opt. Lett.* **29**, 2061 (2004).
- <sup>8</sup>E. Özbay, B. Temelkuran, M. Sigalas, G. Tuttle, C. M. Soukoulis, and K. M. Ho, *Appl. Phys. Lett.* **69**, 3797 (1996).
- <sup>9</sup>W. Y. Zhang, X. Y. Lei, Z. L. Wang, D. G. Zheng, W. Y. Tam, C. T. Chan, and P. Sheng, *Phys. Rev. Lett.* **84**, 2853 (2000).
- <sup>10</sup>J. G. Fleming, S. Y. Lin, I. El-Kady, R. Biswas, and K. M. Ho, *Nature (London)* **417**, 52 (2002).
- <sup>11</sup>S. Y. Lin, J. Moreno, and J. G. Fleming, *Appl. Phys. Lett.* **83**, 380 (2003).
- <sup>12</sup>P. Parimi, W. Lu, P. Vodo, J. Sokoloff, J. Derov, and S. Sridhar, *Phys. Rev. Lett.* **92**, 127401 (2004).
- <sup>13</sup>M. D. Morgan, W. E. Horne, V. Sundaram, J. C. Wolfe, S. V. Pendharkar, and R. Tiberio, *J. Vac. Sci. Technol. B* **14**, 3903 (1996).
- <sup>14</sup>I. Puscasu, G. Boreman, R. C. Tiberio, D. Spencer, and R. R. Krchnavek, *J. Vac. Sci. Technol. B* **18**, 3578 (2000).
- <sup>15</sup>S. J. Spector, D. K. Astolfi, S. P. Doran, T. M. Lyszczarz, and J. E. Reynolds, *J. Vac. Sci. Technol. B* **19**, 2757 (2001).
- <sup>16</sup>A. Jha, *Infrared Technology: Application to Electro-optics, Photonic devices, and Sensors* (Wiley, New York, 2000).
- <sup>17</sup>J. C. McDonald, D. C. Duffy, J. R. Anderson, D. T. Chiu, H. Wu, O. J. A. Schueller, and G. M. Whitesides, *Electrophoresis* **21**, 27 (2000).
- <sup>18</sup>M. Deubel, G. von Freymann, M. Wegener, S. Pereira, K. Busch, and C. M. Soukoulis, *Nat. Mater.* **3**, 444 (2004).
- <sup>19</sup>J.-H. Lee, C.-H. Kim, K. Constant, and K.-M. Ho, *Adv. Mater. (Weinheim, Ger.)* **17**, 2481 (2005).
- <sup>20</sup>J.-H. Lee, C.-H. Kim, Y.-S. Kim, K.-M. Ho, K. Constant, W. Leung, and C. H. Oh, *Appl. Phys. Lett.* **86**, 204101 (2005).
- <sup>21</sup>D. Palik, *Handbook of Optical Constants of Solid* (Academic, Orlando, 1985), pp. 290–295.
- <sup>22</sup>M. Born and E. Wolf, *Principles of Optics* (Pergamon, Oxford, 1980), p. 614.
- <sup>23</sup>Z.-Y. Li and K.-M. Ho, *Phys. Rev. B* **67**, 165104 (2003).